Available online at www.sciencedirect.com
SCIENCE DIRECT®
Journal of Power Sources 128 (2004) 125–134
JOURNAL OF POWER SOURCES
www.elsevier.com/locate/jpowsour

Convenient two-dimensional model for design of fuel channels for proton exchange membrane fuel cells

Falin Chen [a,*], Ying-Zhi Wen [a], Hsin-Sen Chu [b], Wei-Mon Yan [c], Chyi-Yeou Soong [d]

[a] *Institute of Applied Mechanics, National Taiwan University, Taipei 106, Taiwan, ROC*
[b] *Department of Mechanical Engineering, National Chiao Tung University, Hsin-Chu 300, Taiwan, ROC*
[c] *Department of Mechatronic Engineering, Huafan University, Shih-Ting, Taipei 22305, Taiwan, ROC*
[d] *Department of Aeronautical Engineering, Feng Chia University, Seatwen, Taichung 40745, Taiwan, ROC*

Received 6 August 2003; accepted 10 October 2003

Abstract

A theoretical, two-dimensional, along-the-channel model has been developed to design fuel channels for proton exchange membrane (PEM) fuel cells. This has been implemented by solving the resultant ordinary differential equation with a straightforward shooting computational scheme. With such a design tool, an analysis can be made of the effects due to some operation and design parameters, such as inlet velocity, inlet pressure, catalyst activity, height of channel, and porosity of gas-diffusion layer to obtain a fuel cell with high performance. Present results indicate that there is always a trade-off between higher power density and higher efficiency of the fuel cell. Namely, a design for higher power density (a better performance) is always accompanied with a higher fuel efficiency (or a larger fuel consumption rate and a higher fuel cost), and vice versa. When some relevant physical parameters are determined experimentally and applied in the present model, a quantitative design for a fuel cell of either high efficiency or high performance is feasible.

Keywords: Fuel channels; Proton exchange membrane fuel cells; Gas-diffusion layer; Along-the-channel model

1. Introduction

The proton exchange membrane (PEM) fuel cell is an electrochemical device which combines fuel (hydrogen) and oxidant (oxygen) to produce electricity, and water and heat are the major by-products. In past decades, substantial efforts [1–4] have been devoted to reducing the cost as well as promoting the efficiency of the fuel cell. In this respect, the design of high-efficiency fuel channels is one of the important issues [5–19]. Several different types of fuel channels have been used in practical designs, such as straight channels, surpentine channels, and interdigitate channels. The morphology of the channel also varies, namely, meander, spiral or straight types. For a meander or a spiral channel, the length may be several meters long. In such a long channel, the fuel may be entirely consumed before exit, which implies that a certain portion of the cell may not have fuel for chemical reactions. That is, a part of the cell may not produce any electrons during operation and this reduces the efficiency. Therefore, analysis of the channel flow becomes a necessity in fuel cell design and an efficient and convenient theoretical model for channel analysis is essential.

To date, there have been two major approaches for the analysis of channel flow. One uses computational fluid dynamic (CFD) techniques to examine the two- or three-dimensional flow in fuel channels [5–10], the other uses a one-dimensional approximation approach to investigate the variation of flow structure and includes the fuel concentration as well as the current generated along the channel [11–19]. In the CFD approaches, mathematical models are usually developed for the whole PEM fuel cell, which may consider the conservation of mass, momentum and energy, equations governing the electrochemical reaction, and various kinds of physical properties of the components such as diffusivity of the gas-diffusion layer, electro-osmosis in membrane, fuel convection across the membrane, chemical reaction and activity in catalyst layers, and membrane hydration [20–23]. With this approach, however, the computation is rather time-consuming and the analysis procedure is so tedious that the computation of the whole flow field in channels becomes inefficient and is sometimes even an unnecessary step to obtain the fuel cell design.

* Corresponding author. Tel.: +886-2-363-0979; fax: +886-2-363-9290.
E-mail address: falin@spring.iam.ntu.edu.tw (F. Chen).

0378-7753/$ – see front matter © 2003 Elsevier B.V. All rights reserved.
doi:10.1016/j.jpowsour.2003.10.003

Nomenclature

$\tilde{c}$	dimensionless concentration
C	concentration (mol m^{-3})
C_0	inlet concentration (mol m^{-3})
F	Faraday constant (96,500 C mol^{-1})
h	channel height (m)
i	local current density (A m^{-2})
i_0	inlet current density (A m^{-2})
K_i	$i = 1$–5, constants in Eq. (15)
L	channel length (m)
M	molar weight (kg mol^{-3})
n	transferred electron number
P	pressure (Pa)
P_0	inlet pressure (atm)
$\bar{P}$	pressure gradient (Pa m^{-1})
R	universal gas constant (8.314 J mol^{-1} K^{-1})
T	gas temperature (K)
u	velocity in x-direction (m s^{-1})
u_0	inlet velocity in x-direction (m s^{-1})
$\bar{u}$	cross-sectional averaged velocity in x-direction
$\tilde{u}$	dimensionless velocity in x-direction
v	velocity in y-direction (m s^{-1})
V_0	suction velocity (m s^{-1})

Greek letters

α	charge transfer coefficient
γ	reaction order
η	over potential (V)
μ	viscosity (kg m^{-1} s^{-1})
ξ	empirical constant regarding the slip condition at the porous boundary
ρ	density (kg m^{-3})

A more efficient and convenient scheme, which can to some extent reach the goal of fuel cell design both quantitatively and qualitatively, is the channel model [11–19]. Since the flow passes the fuel channel very rapidly, cross-sectional variations of flow structure and other physical parameters such as fuel concentration, fuel density and fuel temperature can be ignored. A major concern is the variation of the relevant physical properties along the channel. It was found that the along-the-channel model is much simplified and that the equations can be solved more conveniently and efficiently. Recently, several along-the-channel models have been developed for the above-mentioned purpose. Nguyen and co-workers [10,11] have proposed a set of governing equations which include water and energy transport across the membrane and have considered heat removal along the channel. Other workers [12–14] have examined the gas dynamics, concentration decay and current drop along the channel. Argyropoulos et al. [15–19] have investigated the pressure drop and the temperature variation along the channel by considering the mass and energy conservation of two-phase flows. In these studies, however, the channel flow was assumed to have a constant velocity along the channel. Under most circumstances, however, this assumption may result in significant discrepancies with reality.

In the present work, a two-dimensional theoretical model is developed, which includes a continuity equation, momentum equations and the Tafel equation. At the bottom of the channel, the consumption of fuel due to chemical reactions is modeled by way of sucking the fuel through the porous boundary. This model allows investigation of the variations of the flow structure, the fuel concentration, and the current density along the channel. A systematic parametric study is implemented to examine the influence of relevant design and operation parameters on the effective length of the fuel channel. Specifically, the effects due to the inlet velocity and pressure and the porosity of the gas-diffusion layer at the bottom can be investigated. The activity of the catalyst attached to the gas diffusion layer can also be analyzed.

2. The theoretical model

A two-dimensional horizontal channel flow is shown schematically in Fig. 1. The channel has a constant height and is sufficiently long that the conditions at both the entrance and the exit do not affect the flow of the domain under consideration. The fluid, either hydrogen in the anode or oxygen in the cathode, is assumed to be an ideal gas. Since the flow velocity is so high, the variation of temperature along the channel is assumed to be negligible. It is also assumed that the bipolar plate in which the fuel channel is built is an ideal collecting electrode with no ohmic loss. The overpotential can then be maintained at a constant value along the channel [12]. As a result, the local current density is a function of the fuel concentration at each specific position [7]. For such a chemically active flow, the continuity equation is:

$$\frac{\partial \rho}{\partial t} + \frac{\partial(\rho u)}{\partial x} + \frac{\partial(\rho v)}{\partial y} = 0, \tag{1}$$

in which $u = u(x, y)$ and $v = v(x, y)$ are the velocity in the x-and y-directions, respectively. Due to the fact that the channel height is very small compared with the channel length, it may be assumed that the density distribution

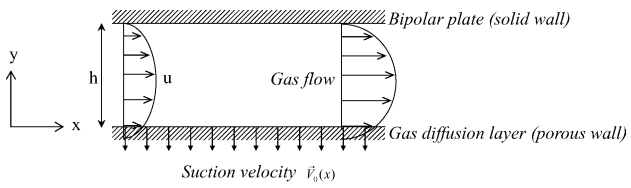

Fig. 1. Schematic description of flow considered. Two-dimensional viscous flow is bounded between bipolar plate (solid wall) at top and gas-diffusion layer (porous wall) at bottom. Velocity profile is essentially a parabolic curve. Because of the porous wall there is a velocity slip at bottom. Because of chemical reaction in the gas-diffusion layer, there is a suction flow across the porous wall, accounted for by suction velocity $\vec{V}_0(x)$.

across the channel is uniform, i.e., $\rho = \rho(x)$. Because $\rho(x) = MC(x)$, Eq. (1) can be converted to:

$$\frac{\partial(Cu)}{\partial x} + \frac{\partial(Cv)}{\partial y} = 0. \tag{2}$$

Integrating Eq. (2) along y and applying Leibnitz's rule gives:

$$C\frac{\partial}{\partial x}\int_0^h u\,\mathrm{d}y + \frac{\mathrm{d}C}{\mathrm{d}x}\int_0^h u\,\mathrm{d}y + C\int_0^h \frac{\partial v}{\partial y}\,\mathrm{d}y = 0. \tag{3}$$

By letting $\bar{u}(x) \equiv (1/h)\int_0^h u(x, y)\mathrm{d}y$ be the averaged velocity over the cross-section of the channel and by applying the non-slip condition at the top $u(x, h) = 0$ and the slip condition at the bottom $u(x, 0) = \xi\bar{u}(x)$, we obtain:

$$h\frac{\mathrm{d}[C(x)\,\bar{u}(x)]}{\mathrm{d}x} = C(x)\,v(x, 0) = -C(x)\,V_0(x), \tag{4}$$

where V_0 is the suction velocity along the bottom of channel, which is defined as $V_0 = (1/nF)(i(x)/C(x))$. Thus, Eq. (4) becomes:

$$\frac{\mathrm{d}[C(x)\,\bar{u}(x)]}{\mathrm{d}x} = -\frac{1}{h}\frac{i(x)}{nF}. \tag{5}$$

The relation between the overpotential η and the electric current density i is governed by the Tafel equation:

$$i(x) = i_0\left[\frac{C(x)}{C_0}\right]^{\gamma}\exp\left(\frac{\alpha F}{RT}\eta\right), \tag{6}$$

so that the suction velocity V_0 can be expressed by:

$$V_0(x) = \left[\frac{1}{nF}\frac{i_0}{C_0^{\gamma}}\exp\left(\frac{\alpha F}{RT}\eta\right)\right]C^{\gamma-1}(x). \tag{7}$$

Note that, the slip boundary condition at the bottom $u(x, 0) = \xi\bar{u}(x)$ is derived from the so-called Beavers–Joseph boundary condition at the interface between a fluid and a porous layer [24], and the parameter ξ essentially accounts for the permeability of the porous media since the factor due to the velocity gradient at the bottom is absorbed into the averaged velocity $\bar{u}(x)$. Given that the velocity gradient does not change significantly along the channel, a change in ξ may be seen as a change in the permeability or, equivalently, a change in the porosity of the porous medium below. In the present study, it considered that ξ varies from 0.1 to 1 [24] due to the fact that the porosity of the gas-diffusion layer at the bottom is high.

For the momentum equation, it is assumed that, for the present two-dimensional channel flow, the velocity in the x-direction is much larger than that in the y-direction. After applying order analysis on the momentum equations (or the Navier–Stokes equations) in both x-and y-directions, a single momentum equation results as follows:

$$\rho(x)\left[u\frac{\partial u}{\partial x} + v\frac{\partial u}{\partial y}\right] = -\frac{\mathrm{d}P}{\mathrm{d}x} + \mu\frac{\partial^2 u}{\partial y^2}. \tag{8}$$

The pressure gradient along the channel is assumed to be constant, i.e., $(\mathrm{d}P/\mathrm{d}x) = \text{constant} = \bar{P}$. Under the normal operating conditions of a 1 kW fuel cell, $\bar{P} = 12\,\mathrm{Pa\,m^{-1}}$ [2,12–14], which is to be used in the present analysis. Integrating Eq. (8) along the height yields:

$$MC\int_0^h\left[u\frac{\partial u}{\partial x} + v\frac{\partial u}{\partial y}\right]\mathrm{d}y = -h\bar{P} + \mu\left.\frac{\partial u}{\partial y}\right|_0^h. \tag{9}$$

To simplify Eq. (9) further, it is assumed that $u(x, y)$ is a quasi-parabolic velocity profile [25] defined as $u(x, y) = A(x)y^2 + B(x)y + G(x)$. At $y = 0$, $u(x, 0) = \xi\bar{u}(x)$ and this leads to $G(x) = \xi\bar{u}(x)$; at $y = h$, $u(x, y) = 0$ and $B(x) = -ha(x) - (\xi/h)\bar{u}(x)$. To obtain $A(x)$, the non-slip boundary condition is applied at the top $u(x, h) = 0$ and this results in $A(x) = -(6/h^2)(1 - (1/2)\xi)\bar{u}(x)$. Consequently the approximated velocity function in x-direction is obtained as:

$$u(x, y) = \bar{u}(x)\left[-6\left(1 - \frac{1}{2}\xi\right)\frac{y^2}{h^2} + 2(3 - 2\xi)\frac{y}{h} + \xi\right]. \tag{10}$$

This equation implies that the horizontal velocity is a second-order parabolic function of y, with a small slip at the bottom of channel, as shown schematically in Fig. 1. To obtain $v(x, h)$, Eq. (10) is substituted in Eq. (8) and the resultant equation is integrated along y and the boundary conditions of v are applied at the top and the bottom of the channel, i.e., $v(x, h) = 0$ and $v(x, 0) = V_0(x)$, yielding:

$$v(x, y) = \frac{[C(x)\,\bar{u}(x)]'}{C(x)}\left[2\left(1 - \frac{1}{2}\xi\right)\frac{y^2}{h^2} - (3 - 2\xi)\frac{y^2}{h} - \xi y\right] - V_0(x). \tag{11}$$

Eqs. (10) and (11) are substituted in Eq. (9) to give the following equation for the channel flow:

$$\left(\frac{2}{15}\xi^2 - \frac{1}{5}\xi + \frac{6}{5}\right)\frac{\mathrm{d}[C(x)\,\bar{u}^2(x)]}{\mathrm{d}x} + \frac{\xi}{h}C(x)\,\bar{u}(x)\,V_0(x) + \frac{\bar{P}}{M} + 12\left(1 - \frac{1}{2}\xi\right)\frac{\mu}{Mh^2}\bar{u}(x) = 0. \tag{12}$$

Eqs. (5), (6) and (12) are the governing equations for the two-dimensional flow along the channel, in which the variations of the fuel concentration $C(x)$, the velocity $u(x)$ and the current density $i(x)$ are to be solved. Since these equations have an initial value problem, the initial velocity at the entrance, u_0, and the initial concentration fed to the channel, C_0, are required. It is therefore assumed that $\tilde{u}(x) = \bar{u}(x)/u_0$ and $\tilde{c}(x) = C(x)/C_0$ and these two relationships are substituted into the equations to give:

$$\frac{\mathrm{d}(\tilde{c}\tilde{u})}{\mathrm{d}x} + K_1\tilde{c}^{\gamma} = 0, \tag{13}$$

$$K_2\frac{\mathrm{d}(\tilde{c}\tilde{u}^2)}{\mathrm{d}x} + K_3 + K_4\tilde{c}^{\gamma}\tilde{u} + K_5\tilde{u} = 0, \tag{14}$$

where

$$K_1 = \frac{i_0}{nFhC_0u_0}\exp\left(\frac{\alpha F}{RT}\eta\right),$$
$$K_2 = \tfrac{2}{15}\xi^2 - \tfrac{1}{5}\xi + \tfrac{6}{5},$$
$$K_3 = \frac{\bar{P}}{MC_0u_0^2}, \qquad (15)$$
$$K_4 = \xi\frac{i_0}{nFhC_0u_0}\exp\left(\frac{\alpha F}{RT}\eta\right),$$
$$K_5 = 12\left(1 - \frac{1}{2}\xi\right)\frac{\mu}{Mh^2C_0u_0}.$$

The initial conditions become $\tilde{u} = 1$ and $\tilde{c} = 1$. These two equations are solved by a fourth order Runge–Kutta scheme. Eqs. (13) and (14) are the two simplified equations for the averaged horizontal velocity $\tilde{u}$ and averaged fuel concentration $\tilde{c}$. After obtaining these two values, the Tafel equation (Eq. (6)) can be applied to obtain the local current density along the channel. The combination of these equations and the shooting scheme becomes a convenient tool to determine various physical parameters relevant to the design of fuel channels of PEM fuel cells. This scheme is different from those developed in other studies [11–19] in which the velocity variations in both *x*- and *y*-directions were ignored and only the effective length was considered. Using this simplified model allows not only the examination of the effective length of the fuel channel under various operation conditions, but also the effects due to relevant design and operation parameters on the fuel cell performance.

3. Typical flow field: an example

Analyses in the present and the following sections are made on the basis of the base case; the values of its relevant physical parameters are shown in Table 1. This case essentially corresponds to a 1 kW PEM fuel cell under normal operation conditions [2,12–14]. The results in terms of the variations of velocity, fuel concentration and current density along the channel are presented in Fig. 2. It is found that the fuel concentration decays monotonically along the channel due to the chemical reaction occurring at the bottom of channel, while the flow velocity increases along the channel because of the depletion of fuel downstream. Both effects are the direct consequence of fuel consumption along the channel, which in turn leads to a decrease in generated current (Fig. 2(b)) because of, again, the depletion of fuel downstream. These findings suggest that variations of these physical properties occur simultaneously, and therefore will be considered as a whole instead of separately as in previous studies [11–19] Also the velocity is taken as constant while the fuel concentration changes along the channel.

The generation of current density decreases along the channel because of the decay in fuel concentration (see Fig. 2(b)). Note that, for the present base case, the fuel concentration decrease by about 50% and the local current density by about 25% within the 10 cm long channel. The variations in these two parameters are very significant for such a short distance, implying that an accurate calculation of the effective channel length cannot be ignored in the design of a high-efficiency fuel cell. In a practical sense, too long a channel will result in a large dead region in the

Table 1
Values of physical parameters of base case corresponding to 1 kW PEM fuel cell [2,12–14].

Channel side	Cathode
Gas flow	Oxygen
Half-reaction	$O_{2(g)} + 4H^+ + 4e^- \rightarrow 2H_2O$
Channel temperature, T (K)	353.15
Inlet gas velocity, u_0 (m s^{-1})	0.1
Inlet gas pressure, P_0 (atm)	2
Inlet gas concentration, C_0 (mol m^{-3})	69.00
Exchange current density, i_0 (A m^{-2})	10^{-5}
Activation overpotential, η (V)	0.3
Reaction order, γ	0.5
Electrons transferred in reaction, n	4
Charge-transfer coefficient, α	2.0
Molar weight, M (kg mol^{-1})	32×10^{-3}
Viscosity, μ (kg m s^{-1})	2×10^{-5}
Channel height, h (m)	10^{-3}
Channel length, L (m)	0.1
Pressure gradient, $\bar{P}$ (Pa m^{-1})	10
Universal gas constant, R (J mol^{-1} K^{-1})	8.314
Faraday constant, F (C mol^{-1})	96500
Slip velocity fraction, ξ	0.1
K_1 (m^{-1})	13.77
K_2	1.181
K_3 (m^{-1})	452.9
K_4 (m^{-1})	1.377
K_5 (m^{-1})	1032.6

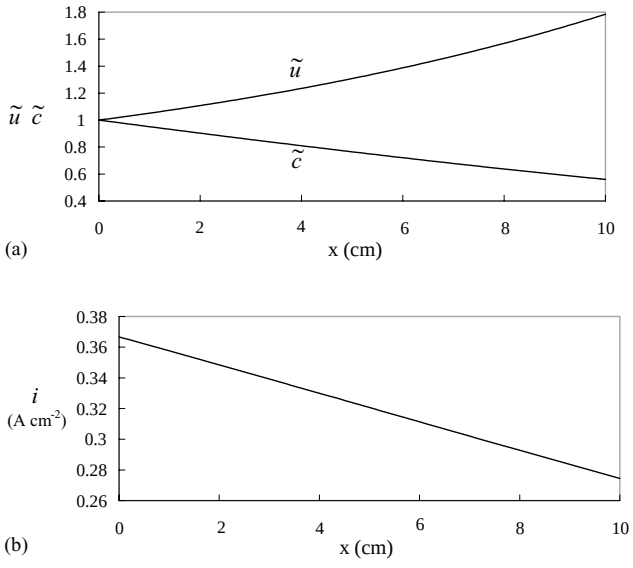

Fig. 2. Along-the-channel variations of major quantities of present problem: (a) dimensionless velocity $\tilde{u}$ and concentration $\tilde{c}$; (b) generated current density. Results are calculated on basis of base case shown in Table 1.

bipolar plate, while too short a channel will cause a great part of the fuel to leave the cell without reaction. A long channel gives a low local current density downstream (or a low performance of the fuel cell) but, with respect of fuel consumption, a long channel length may ensure that the fuel is consumed before leaving the exit. The latter will result in a better efficiency of fuel usage.

4. Physical parameter effects

Several physical parameters have significant effects on the channel flow, which may in turn affect both the design and operation conditions of the fuel cell. These physical parameters include the flow velocity at the inlet, the fuel concentration, the activity of the catalyst, the channel height, and the porosity of the gas-diffusion layer. The following examines the physical effects due to these five parameters with special attention to their influence on the effective length of the channel. When the effect of a particular physical parameter is considered, this parameter will be changed systematically while the other four physical parameters are fixed at the values shown in Table 1.

4.1. Effect of inlet velocity

The variation of flow velocity, fuel concentration and local current density along the channel are shown in Fig. 3(a)–(c),

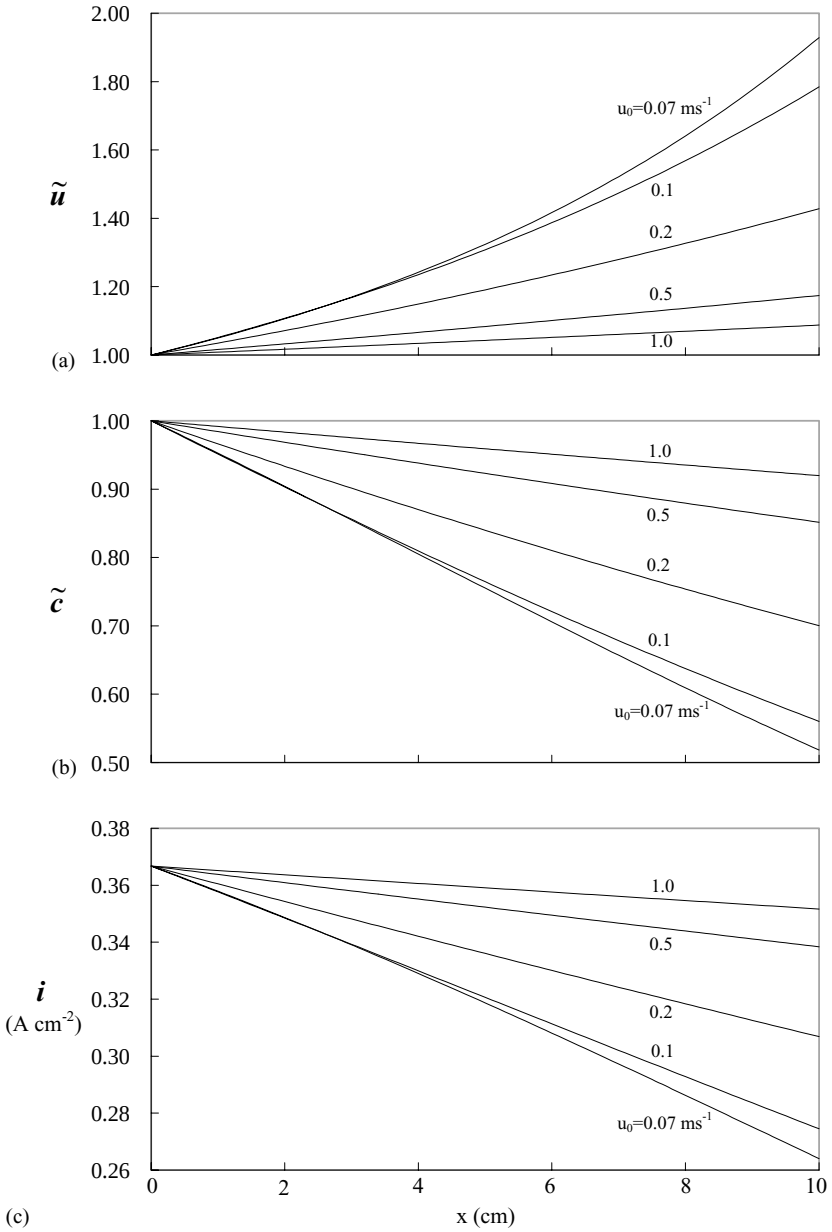

Fig. 3. Effects of inlet velocity on along-the-channel variations of: (a) dimensionless velocity $\tilde{u}$; (b) dimensionless concentration $\tilde{c}$; (c) local current density.

respectively, for variation in inlet velocity from 0.07 to $1\,m\,s^{-1}$. For a lower inlet velocity, because the fuel has more time to diffuse into the active layer at the bottom to react, the fuel concentration decays more rapidly (Fig. 3(b)). Decrease in fuel concentration leads to an increase in flow velocity in accordance with the conservation of mass (Fig. 3(a)) and results in a larger decrease in the local current density due to the higher depletion of fuel or a lower reaction rate (Fig. 3(c)). It is interesting to note that, for an inlet velocity of $1\,m\,s^{-1}$, the changes in flow velocity, fuel concentration and local current density along the channel are all very small. As a result, practically, if a uniformly high current density along the channel (and thus a higher power density) is required, then a larger inlet fuel velocity can be applied to the cell, but at the expense of a higher fuel consumption rate. On the other hand, if the fuel efficiency is the major concern, it is necessary to apply a lower inlet velocity so that the fuel consumption (and thus the reaction) along the channel can be implemented more completely.

4.2. Effect of fuel concentration

From the equation of state of an ideal gas, i.e., $C_0 = P_0/RT$, the fuel concentration is a function of the partial

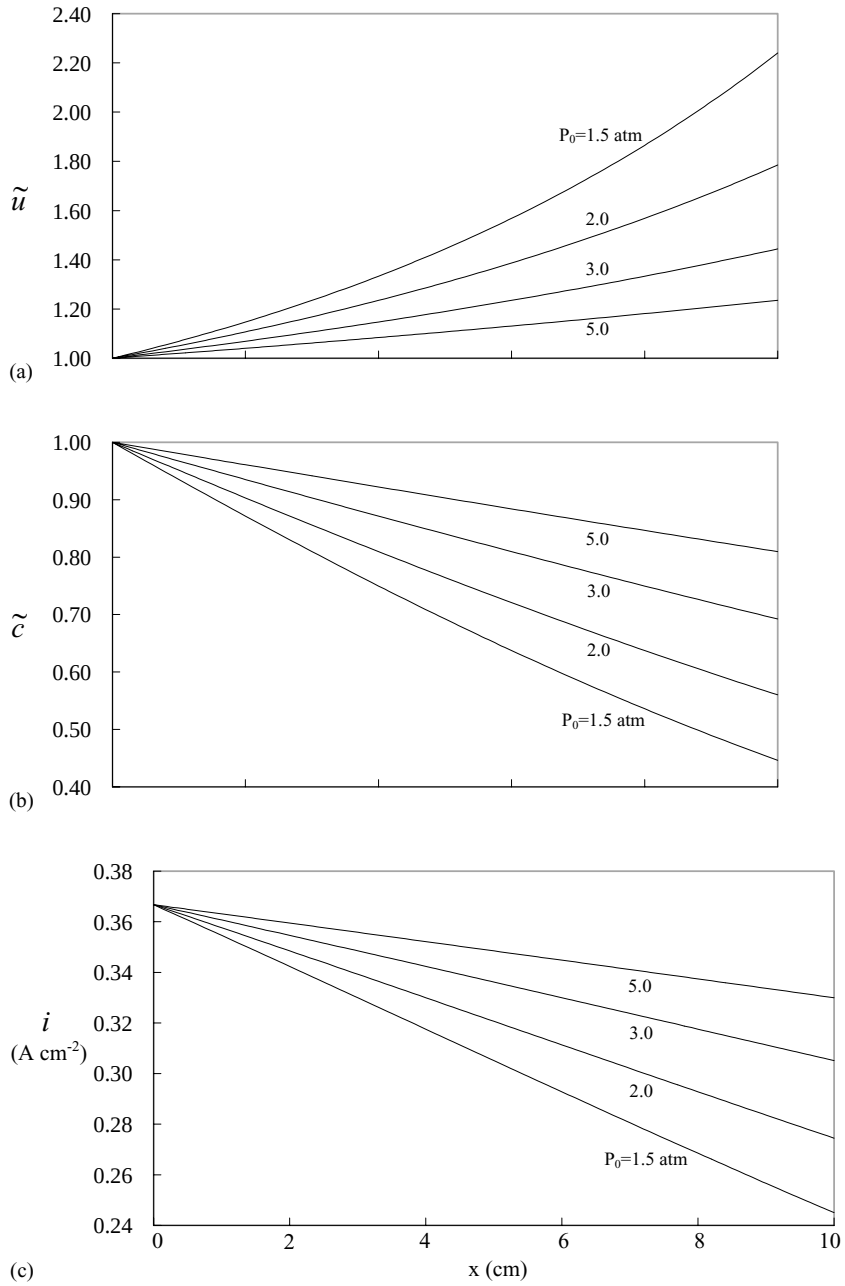

Fig. 4. Effects of inlet fuel pressure on along-the-channel variations of: (a) dimensionless velocity $\tilde{u}$; (b) dimensionless concentration $\tilde{c}$; (c) local current density.

pressure of the fuel gas. Accordingly, the change in fuel concentration can be attributed to the change in partial pressure of the fuel. Thus, to examine the effects of fuel concentration, the inlet pressure P_0 of the fuel was changed from 1.5 to 5 atm. The results are presented in Fig. 4(a)–(c) and show that for a higher inlet pressure (or a higher fuel concentration), and thus a larger pressure gradient along the channel when the pressure at outlet is assumed to be constant, the increase in flow velocity along the channel is smaller (but the overall velocity is higher) (Fig. 4(a)) because the consumption rate of the fuel along the channel is smaller (and the decrease of the fuel concentration along the channel is smaller) (see Fig. 4(b)). Due to the smaller fuel consumption rate, the decrease in current density along the channel is also smaller. As a result, to ensure that the current density along the channel can be uniformly high, or equivalently to have a fuel cell of higher power density, the cell must be supplied with a fuel of higher concentration (a higher inlet pressure) but, again, at the expense of a higher fuel consumption rate.

4.3. Effect of catalyst activity

The activity of the catalyst can be indicated by the value of the overpotential η, which can be converted into the current density i by the Tafel equation (Eq. (6)). The present analysis considers three different activities, corresponding to three

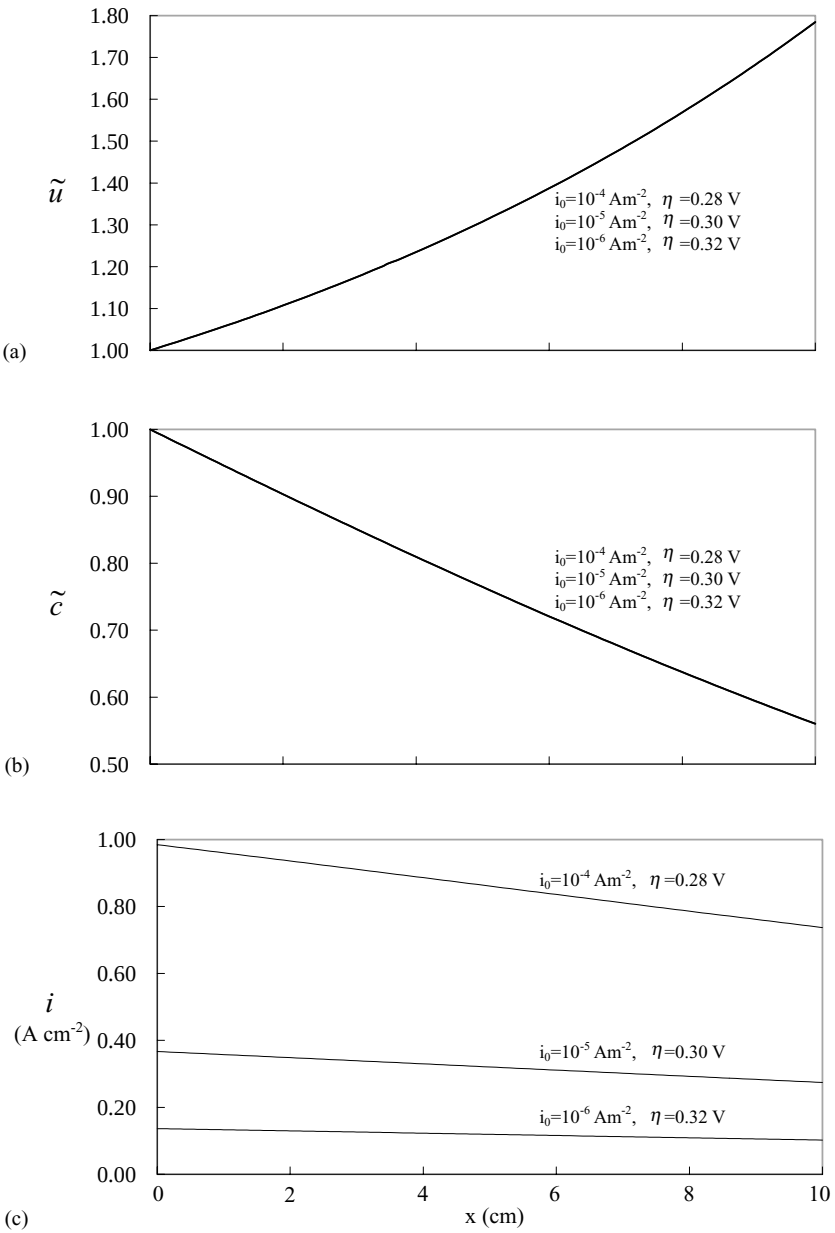

Fig. 5. Effects imposed by different catalysts on along-the-channel variations of: (a) dimensionless velocity $\tilde{u}$; (b) dimensionless concentration $\tilde{c}$; (c) local current density.

overpotentials $\eta = 0.28, 0.30$ and 0.32 V. The corresponding current densities are $i_0 = 10^{-4}$, 10^{-5} and 10^{-6} A cm^{-2}. A catalyst of higher activity leads to a faster reaction rate and thus a faster speed of electron generation and, accordingly corresponds to a lower overpotential loss and a higher current density. Note that, a different catalyst activity implies a different fuel consumption rate, which can be reflected by the change in suction velocity V_0 at the bottom of the channel (see Eq. (7)).

The results shown in Fig. 5(a)–(c) illustrate that the difference in activity of the catalyst examined in the present study does not result in an obvious difference in either the flow velocity (Fig. 5(a)) or the fuel concentration (Fig. 5(b)), because the curves of different activities virtually overlap each other. On the other hand, it has a significant effect on the local current density, as shown in Fig. 5(c), namely: a higher catalyst activity leads to a higher local current density and results in a slightly more rapid decrease along the channel. This indicates that an efficient scheme to raise the fuel cell performance without consuming more fuel is to use a catalyst of higher activity. This is a common scenario accepted by fuel cell researchers world-wide. Accordingly, the development of a high-activity catalyst for PEM fuel cells has been a major research issue, or may be the most important one.

4.4. Effect of channel height

Since it is assumed that the fuel is well mixed across the channel height, a larger height of channel is equivalent to a

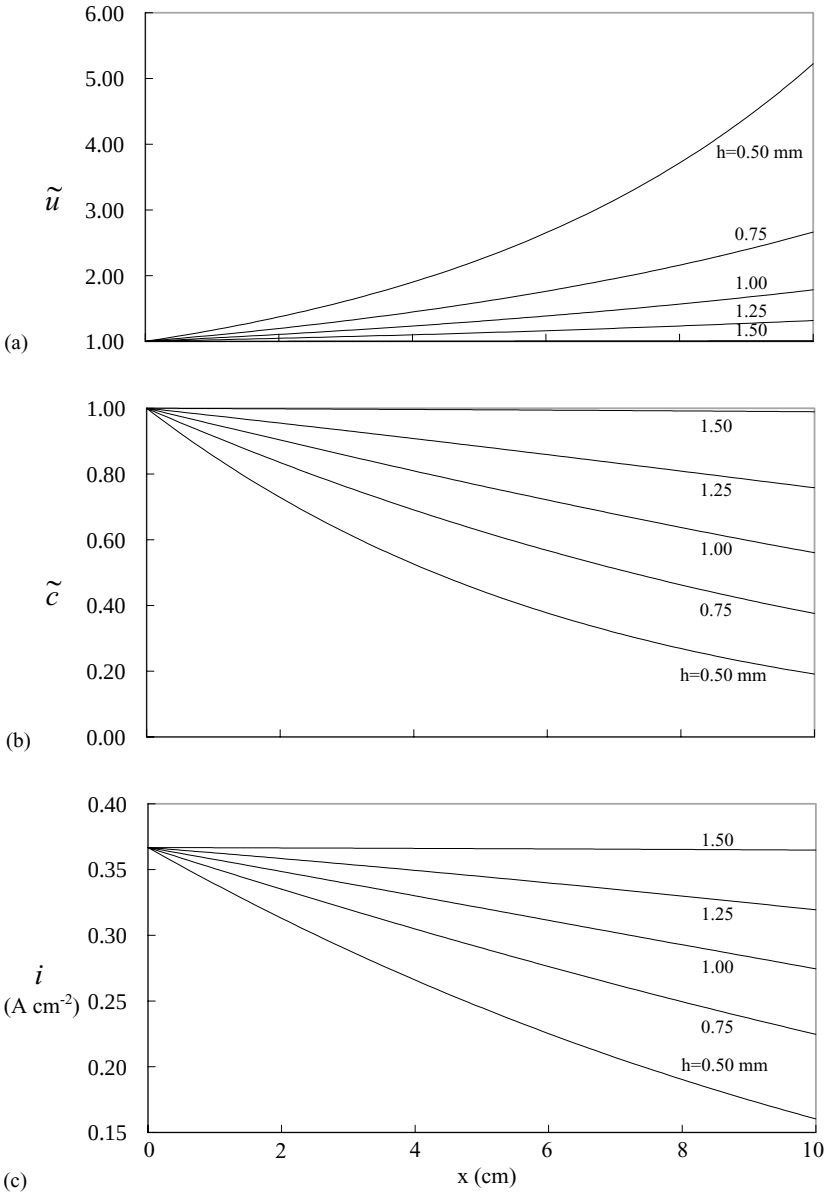

Fig. 6. Effects of channel height on along-the-channel variations of: (a) dimensionless velocity $\tilde{u}$; (b) dimensionless concentration $\tilde{c}$; (c) local current density.

greater mass of the fuel per unit length, or a more sufficient supply of the fuel. Five different heights of channel are considered, viz., $h = 0.5$, 0.75, 1.0, 1.25 and 1.5 mm; the results are shown in Fig. 6(a)–(c). It is seen that a smaller height of channel leads to a larger increase in flow velocity and a larger decrease in fuel concentration along the channel. Alternatively, a smaller height of channel results in a larger decrease of local current density along the channel and thus a smaller power density (or a worse performance) for the fuel cell. Note that, since both the flow velocity and the fuel concentration have been normalized by the corresponding inlet conditions, a larger decrease of fuel concentration in fact accounts for a smaller amount of fuel consumed along the channel. According to these results, the application can be made as follows. To have a fuel cell of higher fuel efficiency, it is necessary to have a larger height of channel because the fuel can be consumed more efficiently. Correspondingly, to have a fuel cell of higher power density, it is necessary to have a larger height of channel so that a larger amount of fuel can be supplied.

4.5. Effect of porosity of gas-diffusion layer

The change in porosity of the gas-diffusion layer can be reflected in the present model by changing the parameter ξ at the bottom boundary. Physically, as mentioned above, a larger ξ means a larger porosity of the gas-diffusion layer. Five cases are considered, namely, $\xi = 0.1$, 0.2, 0.3, 0.5 and 1.0. The results show that a larger ξ (or a larger porosity) results in a smaller increase in flow velocity (Fig. 7(a)) as well as a smaller decrease in fuel concentration (Fig. 7(b)) because a larger portion of fuel is allowed to be sucked into the porous boundary at the bottom due to the larger porosity. Accordingly, a greater chemical reaction occurs in the gas-diffusion layer and leads to a uniformly high current density along the channel (Fig. 7(c)). Accordingly, as discussed

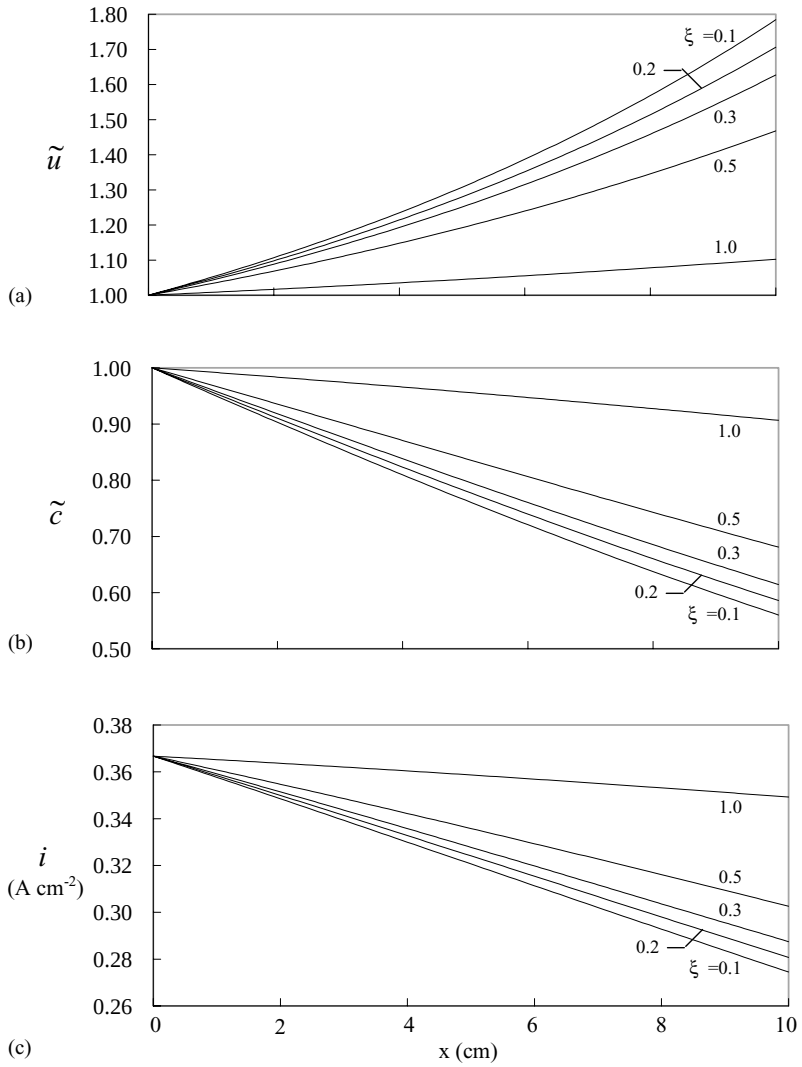

Fig. 7. Effects of porosity of gas-diffusion layer accounted for by parameter ξ on along-the-channel variations of: (a) dimensionless velocity $\tilde{u}$; (b) dimensionless concentration $\tilde{c}$; (c) local current density.

in above, a fuel cell with higher power density requires a larger porosity of the gas-diffusion layer to maintain a uniformly high current density along the channel. This conclusion is consistent with previous analyses of the optimization of the porosity of the gas-diffusion layer ([26],and references wherein)] which show that a higher porosity gives better performance of the fuel cell because in the gas-diffusion layer a larger space (or pores) is given to the water transportation so that the flooding can be prevented in high power density regimes. Thus, a larger porosity of the gas-diffusion layer is preferred for a fuel cell with a high power density.

5. Concluding remarks

A theoretical model for two-dimensional flow in fuel channels has been developed. This allows calculation of variations in fuel velocity, fuel concentration, and current density along the channel. The resultant ordinary equations and the initial conditions at the inlet of the channel consist of an initial value problem, which can be easily solved by a straightforward shooting scheme. The combination of the simplified equation model and the popular shooting scheme becomes a convenient, as well as an efficient, scheme for the design of fuel cell channels, such that several design and operation parameters can be determined for a fuel cell with either high power density or high fuel efficiency.

To have a fuel cell of high power density, results obtained in the present study suggest that it is necessary to: (1) increase the inlet velocity of fuel; (ii) increase the inlet pressure of fuel; (iii) decrease the height of fuel channel; and/or (iv) increase the porosity of the gas-diffusion layer. These four schemes also apply to fuel cell with longer fuel channels (or a larger size). Nevertheless, a high power density is always followed with a high fuel consumption rate, which results in a low fuel efficiency. In other words, to enhance the fuel efficiency of a cell or to apply a fuel cell with shorter fuel channels (or smaller size), it is necessary to apply a lower inlet velocity and/or a lower inlet pressure so that the fuel has a sufficiently long time to react with the catalyst in the gas-diffusion layer at the bottom. With the same reason, a channel with a larger height as well as a gas-diffusion layer with a smaller porosity will also help enhance the fuel efficiency (or shorten the channel length). Results show further that a catalyst of high activity is always most desirable for fuel cell design because it gives a high power density while the accompanied efficiency loss is virtually negligible.

The above conclusions, nevertheless, are made only in qualitative senses; namely, they give only a trend for the design consideration. To obtain useful data for a quantitative design, experiments must be implemented to determine relevant parameters used in the simplified model. Particularly, the value of ξ cannot be determined without going through a series of experiments in which the porosity of the gas-diffusion layer is varied.

Acknowledgements

The authors are grateful for the financial support for this research through the following research grants of National Science Council of Taiwan: NSC 92-2623-7-002-006-ET and NSC 91-2218-E-211-001.

References

[1] T.N. Veziroglu, Int. J. Hydrogen Energy 25 (2000) 1143–1150.
[2] J. Larminie, A. Dicks, Fuel Cell Systems Explained, Wiley, UK, 2000.
[3] P. Costamagna, S. Srinivasan, J. Power Sources 102 (2001) 242–252.
[4] P. Costamagna, S. Srinivasan, J. Power Sources 102 (2001) 269.
[5] A.S. Aricò, P. Cretì, V. Baglio, E. Modica, V. Antonucci, J. Power Sources 91 (2000) 202–209.
[6] D.M. Bernardi, M.W. Verbrugge, AIChE J. 37 (1991) 1151–1163.
[7] D.M. Bernardi, M.W. Verbrugge, J. Electrochem. Soc. 139 (1992) 2477–2491.
[8] T.E. Springer, T.A. Zawodzinski, S. Gottesfeld, J. Electrochem. Soc. 138 (1991) 2334–2342.
[9] T.F. Fuller, J. Newman, J. Electrochem. Soc. 140 (1993) 1218–1225.
[10] T.V. Nguyen, R.E. White, J. Electrochem. Soc. 140 (1993) 2178–2186.
[11] J.S. Yi, T.V. Nguyen, J. Electrochem. Soc. 145 (1998) l149–1159.
[12] A.A. Kornyshev, A.A. Kulikovsky, Electrochim. Acta 46 (2001) 4389–4395.
[13] H. Dohle, A.A. Kornyshev, A.A. Kulikovsky, J. Mergel, D. Stolten, J. Electrochem. Commun. 3 (2001) 73–80.
[14] A.A. Kulikovsky, J. Electrochem. Commun. 3 (2001) 572–579.
[15] P. Argyropoulos, K. Scott, W.M. Taama, J. Chem. Eng. 73 (1999) 217–227.
[16] P. Argyropoulos, K. Scoff, W.M. Taama, J. Chem. Eng. 73 (1999) 229–245.
[17] P. Argyropoulos, K. Scott, W.M. Taama, J. Power Sources 79 (1999) 169–183.
[18] P. Argyropoulos, K. Scott, W.M. Taama, J. Power Sources 79 (1999) 184–198.
[19] P. Argyropoulos, K. Scott, W.M. Taama, J. Chem. Eng. 78 (2000) 29–41.
[20] P. Futerko, I.-M. Hsing, Electrochim. Acta 45 (2000) 1741–1751.
[21] D. Thirumalai, R.E. White, J. Electrochem. Soc. 144 (1997) 1717–1722.
[22] Z.H. Wang, C.Y. Wang, K.S. Chen, J. Power Sources 94 (2001) 40–50.
[23] U.M. Sukkee, C.-Y. Wang, K.S. Chen, J. Electrochem. Soc. 147 (12) (2001) 4485–4493.
[24] G.S. Beavers, D.D. Joseph, J. Fluid Mech. 30 (1967) 197–207.
[25] H.E. Huppert, J. Fluid Mech. 121 (1982) 43–58.
[26] Z. Qi, A. Kaufman, J. Power Sources 109 (2002) 38–46.